Cyclists' exposure to air pollution and noise in Mexico City

Contribution of real-time traffic density indicators integrated into GIS

Philippe Apparicio[1], **Jérémy Gelb**[1], **Paula Negron-Poblete**[2], **Mathieu Carrier**[1], **Stéphanie Potvin**[1], **Élaine Lesage-Mann**[1]

1. *Laboratoire d'équité environnementale, Institut national de la recherche scientifique, Centre Urbanisation Culture Société,*
   385 rue Sherbrooke Est, H2X 1E3, Canada
   {Philippe.apparicio ; jeremy.gelb ; mathieu.carrier ; stephanie.potvin ; elaine.lesage-mann} @inrs.ca

2. *École d'urbanisme et d'architecture de paysage, Université de Montréal*
   2940, chemin de la Côte-Sainte-Catherine, CP 6128 Succursale Centre-ville,
   Montréal, H3C 3J7, Canada
   p.negron-poblete@umontreal.ca

ABSTRACT. Air pollution and road traffic noise are two important environmental nuisances that could be harmful to the health and well-being of urban populations. In Mexico City, as in many North American cities, there has been an upsurge in bicycle ridership. However, Mexico City is also well known for having high levels of noise and air pollution. The purpose of this study is threefold: 1) evaluate cyclists' exposure to air pollution (nitrogen dioxide) and road traffic noise; 2) identify local factors that increase or reduce cyclists' exposure, in paying particular attention to the type of road and bicycle path or lane used; and 3) evaluate the influence of real-time traffic density on cyclists' exposure. A total of 19 bicycle trips made in central Mexico City neighbourhoods were analyzed, representing nearly 11 hours and 137 km. The results of the Bayesian models show that type of road and bicycle infrastructure taken by the cyclist, and proximity to a main artery all have significant impacts on exposure levels. Finally, the variables introduced to control for the traffic encountered by cyclists had a significant positive effect on noise exposure, and a positive but not significant effect on nitrogen dioxide exposure.

RÉSUMÉ. La pollution de l'air et le bruit routier sont deux nuisances environnementales importantes pouvant affecter la santé et le bien-être des populations urbaines. Au même titre que d'autres villes nord-américaines, Mexico assiste à une recrudescence du vélo. Toutefois, Mexico est aussi bien connue pour ses niveaux élevés de bruit et de pollution atmosphérique. Cette étude vise trois objectifs : 1) évaluer l'exposition des cyclistes à la pollution atmosphérique (dioxyde d'azote) et au bruit routier ; 2) identifier les facteurs locaux qui concourent à augmenter ou réduire l'exposition des cyclistes, en accordant une attention particulière aux types de route et de voie cyclable empruntée ; et 3) évaluer l'influence de la densité du trafic en temps réel sur

l'exposition des cyclistes. Au total, 19 trajets à vélo réalisés dans les quartiers centraux de Mexico sont analysés, représentant près de 11 heures et 137 km de collecte. Les résultats des modèles bayésiens montrent que le type de voie routière et cyclable empruntée par le cycliste et la proximité d'une artère principale ont tous des impacts significatifs sur les niveaux d'exposition. Aussi, les variables introduites pour contrôler le trafic rencontré par les cyclistes ont eu un effet positif et significatif sur l'exposition au bruit, et un effet positif, mais non significatif sur l'exposition au dioxyde d'azote.

KEYWORDS: *Cycling, Air pollution, Road traffic noise, GIS, Exposure, Generalized additive mixed models with an autoregressive term, Bayesian modelling, Mexico City.*

MOTS-CLÉS : *pollution de l'air, bruit routier, SIG, exposition, modèles additifs généralisés mixtes avec un terme autorégressif, modèles bayésiens, ville de Mexico.*

1. Introduction

Cycling is an increasingly popular means of transportation in many North American and European cities (Buehler and Pucher, 2012; Pucher *et al*., 2011). This trend is also being seen in many cities in the South, especially in Latin America (Ríos Flores *et al*., 2015; Rosas-Satizábal and Rodriguez-Valencia, 2019; Tucker and Manaugh, 2018). This is the case in Mexico City, where the number of utility cyclists has considerably risen in recent years. According to the most recent origin-destination study (Ciudad de México, 2017), the modal share of cycling in Mexico accounts for 2.2% of all weekday travel in the metropolitan area (1.6% in Mexico City). In 2016, 158,524 bicycle trips were made every day in Mexico City (Ciudad de México, 2017): that is, three times the number of the year before. This huge increase is the direct result of Mexico City's bicycle mobility strategy (Gobierno del Distrito Federal, 2011, 2017), which is intended to promote bicycle ridership within a dynamic of intermodality. In 2010, therefore, the city developed a public bike sharing system called Ecobici, featuring a fleet that has continued to grow ever since. In 2018, the system consisted of 480 stations and 6,800 bicycles spread over 38 km^2. In the past decade, Mexico City has built cycling infrastructures comprised of both off- and on-street bicycle paths and bike lanes. The length of the cycling paths has expanded from only 72 kilometres in 2008 to 170 kilometres in 2016. There are also two very large parking areas (each offering more than 400 spaces for bicycles), 2,057 bike docking points, including 1,293 in public transit stations, and 29 repair stations (Ciudad de México, 2017). It has been widely shown that cycling infrastructure increases the proportion of cyclists while augmenting their safety (Dill and Carr, 2003; Pucher *et al*., 2011; Teschke *et al*., 2012). Awareness-raising activities also help to promote bicycle ridership in the city. Since 2007, every Sunday, cyclists have been able to enjoy a route of about 50 kilometres along the city's main arteries that is exclusively devoted to them. In 2010, themed night trips on certain holidays were also added. Finally, free training in bicycle mechanics and traffic regulations is offered to adults and children wishing to acquire the knowledge to allow them to safely cycle to work or school. These factors combined with Mexico City's recurrent car traffic congestion problems (Leo *et al*., 2017), are helping to make utility

cycling more and more attractive in the city, even though the use of cars still largely predominates.

The individual and collective benefits of urban cycling are now well-known and widely documented in the literature (Bigazzi and Figliozzi, 2014; Fishman *et al*., 2015; Rojas-Rueda *et al*., 2011). For individuals, cycling increases physical activity levels, thus improving cardiovascular health while reducing the risks of chronic illnesses and some types of cancer, as well as of overweight and obesity (Bassett *et al*., 2008; Oja *et al*., 1998; Woodcock *et al*., 2009). Collectively speaking, this translates into a reduction in healthcare costs, as well as in road congestion, noise, and greenhouse gas emissions (Hatzopoulou *et al*., 2013; Rojas-Rueda *et al*., 2011).

Despite these positive spin-offs, urban cycling is also associated with health risks, due to potentially high levels of exposure to air pollution, noise, and road traffic. In a recent systematic review, Cepeda *et al*. (2017) concluded that motorists and public transit commuters have higher levels of exposure than cyclists and pedestrians. However, because of their higher levels of ventilation, cyclists inhale more pollutants. For example, a recent study conducted in Montreal (Canada) showed that inhaled doses of the nitrogen dioxide (NO_2) pollutant are 3.79 higher for cyclists than for motorists during rush hour (Apparicio *et al*., 2018). Nevertheless, several studies have demonstrated that the benefits of urban cycling would appear to largely surpass the risks (De Hartog *et al*., 2010; Rojas-Rueda *et al*., 2011). Moreover, the air pollution risks in extreme air pollution concentrations may outweigh the benefits of physical activity in fewer than 1% of cities across the globe (Tainio *et al*., 2016).

Because of the benefits and risks associated with urban cycling, it is not surprising that many studies have analyzed cyclists' exposure to air pollution and, more rarely, noise in a number of cities around the world. However, a recent systematic review on exposure to road traffic-generated air and noise pollution have shown that there has been little analysis of cities in the South (Khan *et al*., 2018): out of 57 articles selected, European and North American cities are by far overrepresented, compared with cities in the South, which only include four case studies (Macau and Beijing in China, Seoul in Korea, and Delhi in India).

The aim of this article is thus to contribute to our understanding of cyclists' exposure to noise and air pollution in cities in the South by exploring the case of Mexico City. More specifically, the present study has three objectives. The first is to simultaneously evaluate cyclists' exposure to noise and to NO_2 pollutant during trips made in central city neighbourhoods, something that few studies have done to date (Apparicio *et al*., 2016; Apparicio *et al*., 2018; Boogaard *et al*., 2009; Gelb and Apparicio, 2020). The second objective is to identify local factors that increase or reduce cyclists' exposure, in paying particular attention to the type of road and bicycle path or lane used, proximity to main arteries, and travel speed and slope. After controlling for these factors, the third objective is to evaluate the influence of real-time traffic density on cyclists' exposure.

2. Materials and methods

2.1. Study design and routes

The study area is the main city in the Mexican metropolitan region, Mexico City, a metropolis of 8.9 million inhabitants. Several of its geophysical and meteorological characteristics foster high levels of pollution. On the one hand, the city is situated at 2,240 metres above sea level and is surrounded by a chain of mountains, "favoring the transformation of primary pollutants into ozone and other oxidants" (Vallejo *et al.*, 2004). Added to this is the lack of rain during the long winter dry season (from November to March), which does not encourage the cleansing of fine particles from the air (Ouyang *et al.*, 2015).

Bicycle trips were made from February 27 to March 3, 2017 (Figure 1) in five districts of Mexico City (Miguel Hidalgo, Cuauhtémoc, Álvaro Obregón, Benito Juárez and Coyoacán). Only one person (a professor of urban studies) made the trips. He was assisted by an urban studies student who followed him on a bicycle for safety reasons. The two participants cycled together and followed the routes on their cellphones using Google MyMaps. This study has been approved by the Institutional Review Board (Ethical Review Board of Institut national de la recherche scientifique) (Project No CER-15-391).

The routes were previously defined using Google MyMaps by a professor of urban planning and represent hypothetical links between various residential neighbourhoods and several main destinations in the city. The destinations selected are either important employment centres (*e.g.* Polanco, an office and business district), major shopping destinations (*e.g.* the historical centre), or centres of higher education (*e.g.* Universidad Nacional Autónoma de México's main campus – CU). Moreover, when designing the routes, we were careful to select a variety of roads, streets, and bicycle paths and lanes.

After cleaning up the data (elimination of trips due to a defective device), 19 trips were retained, representing nearly 11 hours and 137 km (Figure 2). Note that each trip
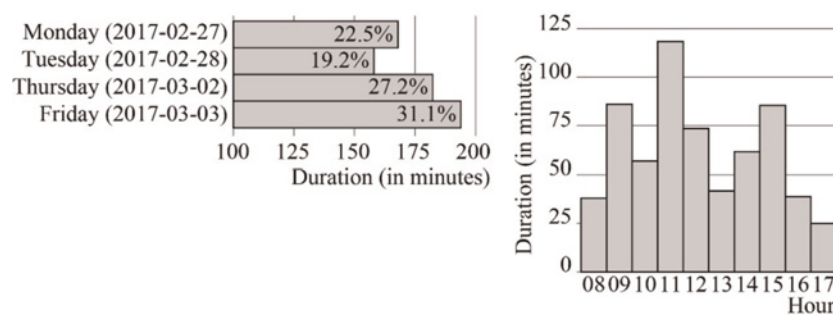
Figure 1. Days and times of data collection

① Chapultepec park   ④ Frida Kahlo Museum
② Historical centre   ⑤ Polanco
③ Universidad Nacional Autónoma de México
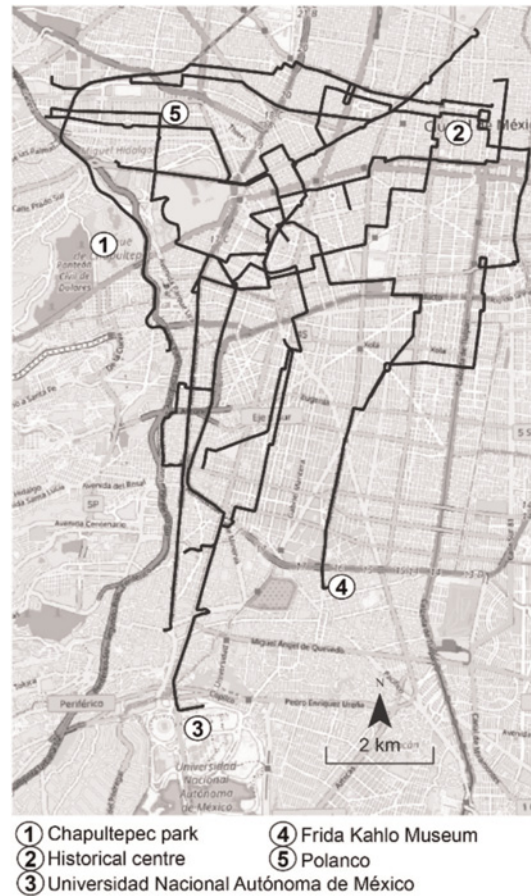
Figure 2. Sample routes

was cycled once. On average, a trip was about half an hour and seven kilometres long, with a speed of 13.11 km/h (Table 1).

The GPS tracks were map-matched to the OpenStreetMap (OSM) street network data (Contributors OpenStreetMap, 2017) by using the OSRM API (Luxen and Vetter, 2011). The results of the map-matching for each trip were then validated by using the videos that we took and modified as needed in QGIS. This validation step is necessary because the GPS localization is sometimes not accurate enough to decide whether the point belongs to a road or a bicycle lane just alongside. The map-matching process is described more in depth in a previous article (Apparicio *et al*., 2019). Note that only the location of GPS points was changed during the map-matching process, time and speed reported by the GPS watches were not modified. Overall, the modifications were minor. The traces were cut as 1-min segments (temporal resolution of the sensors) and all the measurements were assigned to these segments by using timestamp.

Table 1. Summary statistics for the 19 trips

	Route length (in km)	**Route duration (in minutes)**	Speed (km/h)
Minimum	5.421	22.55	11.02
first quartile	5.961	27.77	12.26
Median	6.612	29.88	13.48
Third quartile	8.587	38.73	13.78
Maximum	10.477	51.18	14.62
Mean	7.177	32.94	13.11
Standard deviation	1.759	7.80	1.12
Sum	136.354	625.77	–

The use of the OSM street network data offers two main advantages. First, it contains two keys for identifying the types of roads or streets (key:*highway*) and types of bicycle paths or lanes (key:*cycleway*). Second, because the OSM data is available for most cities around the world, it facilitates comparisons between cities regarding the impact on air pollution and noise exposure of the type of road and bicycle path or lane taken by the cyclist (Apparicio and Gelb, 2020; Gelb and Apparicio, 2019, 2020). The tags used to describe the OSM features are standardized and their detailed description is available in the OSM's documentation online. Despite this standardization effort, one can expect some differences between cities considering the presence of specific infrastructure and the characteristics of the local community of contributors (Hall *et al*., 2001; Mooney and Corcoran, 2012). In this study, according to the first OSM key, several types of roads were taken by the cyclist: trunk (i.e. most important roads; *e.g*. avenida Revolución), primary (e.g. avenida Insurgentes Sur; paseo de la Reforma), secondary (*e.g*. avenida Horacio), and tertiary (*e.g*. avenida Michoacán) roads; residential and pedestrian (*e.g.* within Chapultepec park) streets; and cycleways (Figure 3). During the routes, the cycleways taken were primarily on-street bicycle paths and, secondarily, off-street bicycle paths and bike lanes (Figure 4).

2.2. Measurements of individual exposure

2.2.1. Exposure to air pollution (NO_2) and noise

We realized a mobile data collection using four types of devices: 1) an Aeroqual Series 500 Portable Air Quality Sensor (Auckland, New Zealand), 2) a
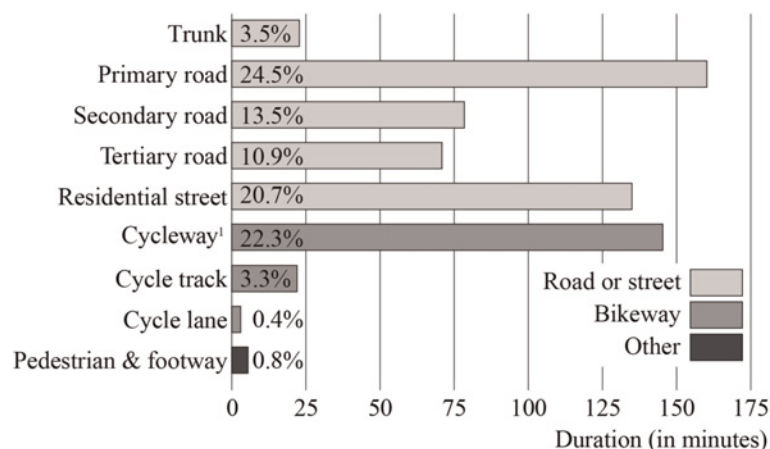
¹ The type cycleway type includes on- and off-street bicycle paths.

*Figure 3. Types of roads, streets, and bicycle paths and lanes taken during
the routes*

Brüel & Kjaer Personal Noise Dose Meter (Type 4448 – class 2, Narum, Denmark), 3) a Garmin GPS watch (910 XT, Olathe, KA, USA), and 4) a Garmin Virb action camera (Olathe, KA, USA).

The Aeroqual devices have two sensors – nitrogen dioxide (NO_2) and temperature and humidity sensors – that record the average NO_2 value (μg/m^3), the temperature in degrees Celsius, and the percentage of humidity every minute. According to the Aeroqual supplier's product information, the NO_2 sensor has the following characteristics: range (0-1 ppm), minimum detection (0.005 ppm), accuracy of factory calibration ($< \pm 0.02$ ppm   0-0.2 ppm; $< \pm 10\%$ 0.2-1 ppm),   and   resolution (0.001 ppm). The NO_2 sensors used were pre-calibrated by the supplier before the data collection. As recommended by the manufacturer, we let them run during 24 h the day before the data collection, and 1 h (warmup) every morning before starting the trips. The device was fixed to a harness on the right shoulder of the participant, as close as possible to the breathing area. As pointed out by several authors (Gelb and Apparicio, 2020; Morawska *et al*., 2018; Snyder *et al*., 2013), the use of these low-cost portable air quality devices is particularly interesting for mobile data collection. This explains why Aeroqual Series 500 monitors have largely been used in numerous studies on individual exposure or air pollution mapping, *e.g.* (Apparicio *et al*., 2016; Apparicio *et al*., 2018; Delgado-Saborit, 2012; Deville Cavellin *et al*., 2016; Gelb and Apparicio, 2020; Minet *et al*., 2017). In urban areas, vehicular exhaust along transportation networks is the primary source of ambient pollution, including nitrogen oxides (NOx) (Crouse *et al*., 2009). Exposure to high concentrations of transport-related air pollutants, such as nitrogen dioxide, can lead to increase in respiratory difficulties and asthma (Costa *et al*., 2014; Khaniabadi *et al*., 2017).

Off-street bicycle path

On-street bicycle path

Cycle lane

Photo credit source: First author.

Figure 4. Examples of bicycle paths in Mexico City

The Brüel & Kjaer devices record the average decibel levels (dB(A)) per minute ($L_{aeq,1\ min.}$) with the following characteristics: exchange rate (3 dB), sound level range (certified 65-140 dB, reliable down to 58 dB), accuracy (±2 dB). That means a difference of 3 dB(A) corresponds to a doubling of noise intensity. As recommended by the manufacturer, the personal Noise Dose Meter (Type 4448) was calibrated once a day using the Sound Calibrator Type 4231 (calibration accuracy ±0.2 dB). A temporal resolution of 1 min for both the Aeroqual monitor and the Brüel & Kjaer Noise Dose Meter is sufficiently detailed considering that with a mean speed of 15 km/h, a cyclist

can ride only 250 m. The Garmin watch's data logging was set every second to obtain a GPS trace and the cyclist's speed that were as accurate as possible. The clocks of all devices (air pollution monitors, noise dose meters, and GPS watches) were synchronized every morning during the data collection.

2.2.2. Exposure to road traffic

The Garmin Virb action camera was attached to the bicycle's handlebars, thereby enabling to obtain the cycling trip video. We were then able to estimate, in a relatively accurate manner, the traffic encountered along the route. We were looking for the numbers of moving cars and heavy vehicles (trucks and buses), the numbers of stopped cars and heavy vehicles with their engines running. We used our internally developed software to perform the counting (Apparicio *et al.*, 2021). This application is quite simple and allows the user to watch a video and click on it when particular events occur. By holding a predefined key, the user can separate events into categories (in this case, moving car, stopped car, moving truck, or stopped truck). The time and location on the screen of events are recorded and saved in JSON files. To validate the process, two students counted the vehicles for each video, and we then compared their results. For each minute of a trip, two indicators are reported: the overall counting concordance (Equation (2)) and the category-wise concordance (Equation (3)). These indicators can be read as the percentage of concordance between users. For example, with two participants, *Ctotal* represents the number of vehicles counted by the two participants per minute, and *Cdiff* is the absolute difference between the two counts per minute:

$$OCC = \frac{C_{total} - C_{diff}}{C_{total}}, \text{ with}$$
$$C_{total} = \sum_{i=1}^{I} \sum_{n=1}^{N} C_{ni} \text{ and } C_{diff} = \sum_{n=1}^{N} |C_{ni} - C_{ni2}| \text{ for each pair in N.}$$
(1)

The same principle can then be applied in considering the different categories; $C_{diffcat}$ is then the absolute difference for each category between the two counts per minute:

$$Cwx = \frac{Cti_{total} - Cti_{diff}}{Cti_{total}}, \text{ with}$$
$$C_{total} = \sum_{i=1}^{I} \sum_{n=1}^{N} C_{ni} \text{ and } C_{diff} = \sum_{n=1}^{N} \sum_{t=1}^{T} |C_{ntii} - C_{nti2}| \text{ for each pair in N.}$$
(2)

with C_{nti} representing the number of events of type t counted at minute n by participant i, for N minutes, T types of event and I participants. For each trip, the average of these two indicators could then be computed. This average was also weighted by the number of events encountered per minute in order to give greater importance to minutes with more events.

2.3. Statistical analyses

All statistical analyses were conducted using R for statistical computing software version 3.6.1 (Team R Core, 2017). First, summary statistics are reported to describe the measures of exposure to noise (dB(A)) and air pollution (NO_2) per minute. Next, three Bayesian models were developed using the *brms* package (Bürkner, 2017, 2018), in which the dependent variables are the level of noise exposure and the level of NO_2 exposure, and the observations are the one-minute segments (N = 630).

The models proposed here are largely based on recent studies (Apparicio and Gelb, 2020; Gelb and Apparicio, 2019, 2020): GAMMAR models (generalized additive mixed models with an autoregressive term) (Wood *et al.*, 2016) with a student distribution for the dependent variable. Consequently, four types of terms were introduced into each model: random effects terms, non-linear terms (*i.e.* splines), an autoregressive term, and fixed linear terms. Moreover, the independent variables introduced into the model can be grouped into six categories (Table 2).

Firstly, the road traffic noise and air pollution could vary according to day of the week, time of day, and location (Apparicio *et al.*, 2016; Dons *et al.*, 2012). Hence, the day of the week was introduced into the three models as a random effect, and the time of day (number of minutes passed since 08:00) as a non-linear term (*i.e.* spline) (Apparicio and Gelb, 2020; Gelb and Apparicio, 2019, 2020). A moving average term (MA = 3) was used to control the temporal autocorrelation because consecutive observations are more likely to be similar than observations selected randomly. As done previously (Apparicio and Gelb, 2020; Gelb and Apparicio, 2019, 2020), geographic coordinates were also introduced as non-linear terms (*i.e.*, bivariate spline) to control the spatial autocorrelation. It should be noted that these three terms are introduced in the model to control for various forms of pseudo-replication (temporal and spatial autocorrelation). Consequently, they will not be analyzed in detail.

Secondly, continuous variables – *i.e.* fixed linear terms – are related to weather conditions: temperature (in Celsius) and humidity (%) measured by the Aeroqual sensor. Thirdly, speed (km/h) and slope (%) are introduced. Slope was obtained from SRTM (Shuttle Radar Topography Mission) elevation data version 4.1 (Jarvis *et al.*, 2008; Reuter *et al.*, 2007) and was calculated as the difference between the starting and ending points of the segment.

Fourthly, we looked at the time spent (in minutes) on the different types of roads, bicycle paths or bike lanes (see Figure 3). It is worth noting that if the cyclist used a bike lane, we calculated both the time spent on the bike lane as well as the time spent on the type of road with the bike lane. Fifthly, bicycle paths were used (totally or partially) for more than one quarter of the 630 one-minute segments (167, 26.5%). Since a bicycle path's (on- or off-street) proximity to the closest section of road can have a significant impact on the levels of exposure and inhalation, we constructed several dummy variables to evaluate the impact of these major types of roads within a distance of 25 metres: highway (n = 23, 13.8%), trunk (n = 72, 43.3%), primary road (n = 74, 44.3%), and secondary road (n = 94, 56.3%).

Table 2. Summary statistics for the 19 trips

Statistic	Min	Q1	Q2	Mean	Q3	Max	SD
Temperature (C)	15.55	21.23	25.28	23.95	27.25	31.17	4.23
Humidity (%)	17.32	20.96	26.03	31.39	39.12	58.00	12.67
Km/h	0.00	8.52	12.77	12.35	16.75	24.02	5.52
Slope (%)	-15.76	-0.92	0.00	0.01	1.15	17.86	2.95
Intersections crossed (n)	0.00	1.00	2.00	2.40	3.00	10.0	1.75
Total cars encountered (n)	0.00	17.00	32.00	36.25	51.00	166.00	24.98
Total heavy vehicles encountered (n)	0.00	1.00	2.00	3.22	5.00	27.00	3.31
Moving cars encountered (n)	0.00	10.00	21.00	26.54	37.00	153.00	21.89
Moving heavy vehicles encountered (n)	0.00	0.00	1.00	2.01	3.00	20.00	2.32
Trunk road (min.)	0.00	0.00	0.00	0.04	0.00	1.00	0.18
Primary road (min.)	0.00	0.00	0.00	0.26	0.57	1.00	0.42
Secondary road (min.)	0.00	0.00	0.00	0.14	0.00	1.00	0.40
Tertiary road (min.)	0.00	0.00	0.00	0.11	0.00	1.00	0.30
Residential street (min.)	0.00	0.00	0.00	0.21	0.16	1.00	0.39
Pedestrian path or footway (min.)	0.00	0.00	0.00	0.01	0.00	1.00	0.09
Cycleway (min.)	0.00	0.00	0.00	0.23	0.20	1.00	0.41
Bike lane (min.)	0.00	0.00	0.00	0.04	0.00	1.00	0.18

Sixthly, we controlled the impact of the real-time traffic density. For the NO_2 exposure model, we used the number of cars and heavy vehicles (trucks and buses), moving or stopped, encountered per one-minute segment. For the noise exposure model, we only introduced the number of moving cars and moving heavy vehicles. The above two measures were obtained by analyzing the videos as described in the previous section. Priors used for the Bayesian models (Gelman, 2006; Gustafson *et al*., 2006) are reported at Table S1 (supplementary material).

To meet the third objective – evaluate the influence of real-time traffic density on cyclists' exposure – , two different models were estimated. For each pollutant (NO_2 and noise exposure), a first model is built with the control variables (i.e. day of the week, time of day, location, weather conditions, slope and speed) and the predictors related to the type of road and bicycle path taken by the cyclist. In a second model, the predictors related to real-time traffic density are added.

2.4. Spatial Data Processing and Analysis

Figure 5 summarizes the spatial data processing and analysis based entirely on open-source solutions (Python, Java, OpenStreetMap, OSRM et R). Briefly, the data from the different sensors is structured and imported into an SQLite database (SpatiaLite) by using a Python script (step 1). Next, all the datasets are merged by using the time stamp. This results in a *point shapefile* representing the seconds of each trip and containing the values of nitrogen dioxide, road traffic noise (dB(A)), temperature, humidity and the link to the image extracted from the video (step 2). These data are then map-matched on the OpenStreetMap network by using the OSMR API and the validation of that process is carried out using the images extracted from the videos (step 3). As mentioned before, the real-time traffic density indicators are built in *Vifeco* (a Java Application) and exported into JSON files with two attributes: categories of vehicles (moving or stopped cars/heavy vehicles) and the time elapsed since the beginning of the video (step 4). The final geographic files are obtained by merging the map-matched data, OpenStreetMap data and the real-time road traffic data (step 5). Finally, these *shapefiles* are imported and analyzed in R with the *Rgdal* and *brms* packages.

3. Results

3.1. Univariate statistics: Levels of air pollution and road traffic noise exposure

The noise levels measured during the trips vary substantially, ranging from 61.4 to 90.5 dB(A) ($L_{Aeq,1\ min}$) (Table 3). The World Health Organization (WHO) group identified two priority health outcome lines of evidence for road traffic noise (World Health Organization, 2018). The first threshold value of 53.3 dB for the average road traffic noise exposure during the day (L_{den}) corresponds to an absolute risk of 10% for the prevalence of a highly annoyed population. The second one of 59.3 dB (L_{den}) corresponds to an increase of 5% of the relative risk for the incidence of ischemic heart
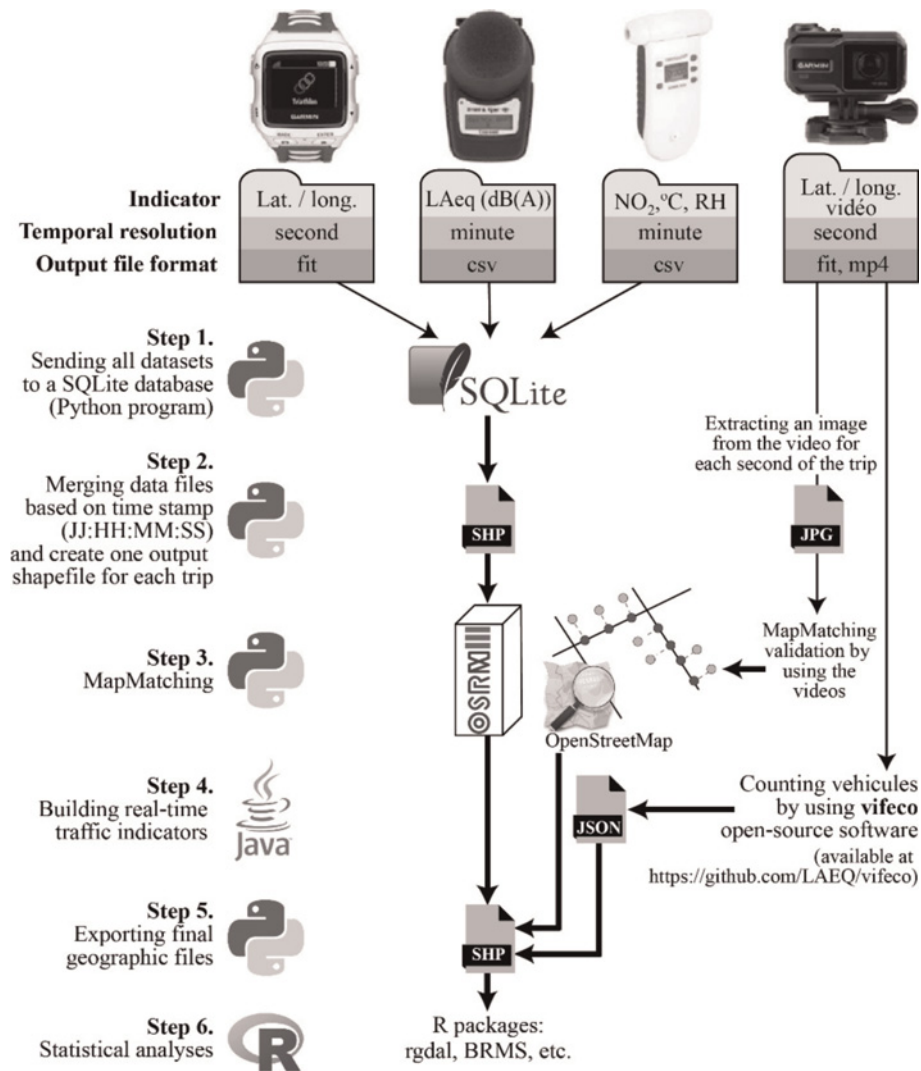
Figure 5. Spatial data processing and analysis

disease. In addition, the Secretariat of the Environment and Natural Resources of Mexico recommends that noise should not exceed 65 dB(A) ($L_{Aeq\ 24h}$) during the day (Secretaría de Medio Ambiente y Recursos Naturales, 2013). The levels of noise measured in Mexico City are therefore relatively high, with mean and median values above the 70 dB(A) threshold. In looking at the values of the percentiles, we see that, for 95% of the times that the cyclist spent on the trips, the noise values exceeded the guideline value of the Secretariat of the Environment of Mexico (P5 = 65.32).

NO$_2$ pollution varies from 54 to 394 μg/m^3, with mean and median values of 219 and 223 μg/m^3 respectively (Table 3). The pollution levels found are mostly higher than 200 μg/m^3, the WHO short-term (1-hour) NO$_2$ guideline value (World Health Organization, 2006). Moreover, for close to 10% of the times spent on the bike, the participant was even exposed to values that exceeded 300 μg/m^3 (P90 = 294.4; P95 = 327.8). These results must be interpreted with caution. They are raw data coming

Table 3. Descriptive statistics for the exposure variables per minute

Statistic	$L_{\text{Aeq, 1 min}}$(dB(A))	NO$_2$ (μg/m^3)
Mean[a]	74.8	218.60
Standard deviation[a]	8.8	62.91
Percentiles		
1	63.2	97.6
5	65.3	114.2
10	66.5	131.7
25	69.2	170.2
50	71.9	222.7
75	75.1	261.9
90	77.9	294.4
95	79.7	327.8
99	82.8	365.6
ACF with		
k = 1	0.45	0.94
k = 2	0.16	0.87
K = 3	0.15	0.85
Moran I	0.28 (d = 250)	0.61 (d = 300)

Note: to calculate Moran's I statistic, we used a binary matrix and defined as neighbors of the segment *i* all the segments in a buffer of length *d* around *i* with *d* ranging from 50 to 500m with a step of 50m. Only the highest values are here reported. [a]Mean and SD of dB values are computed using the *seewave* package (Sueur *et al.*, 2008). These values are raw data and must be interpreted with care, especially the NO$_2$ values which probably overestimate the real individual exposure because the Aeroqual NO$_2$ sensor is known for its cross-sensitivity to ozone (O$_3$).

Table 4. Concordance between the counts

	Overall counting concordance	Category wise concordance
Minimum	91.32	85.47
Maximum	96.38	91.24
Median	94.86	90.66
Standard deviation	1.14	2.26

from a low-cost sensor and could overestimate real exposure, especially because the Aeroqual NO_2 sensor is known for its cross-sensitivity to ozone (O_3) (Lin *et al.*, 2015).

The NO_2 and noise exposure are characterized by strong temporal and spatial autocorrelations (see ACF and Moran I values, Table 3). This justifies introducing a moving average and a spline on the geographic coordinates in the three models. As found previously (Apparicio *et al.*, 2016; Gelb and Apparicio, 2020), there is no correlation between the two measures of exposure (Pearson's correlation coefficient = 0.003, P = 0.86).

3.2. Univariate statistics: Levels of air pollution and road traffic noise exposure

In order to introduce real-time traffic density into the Bayesian models as independent variables, it is appropriate to verify the agreement between the two evaluators who assessed the vehicle counts. To this end, univariate statistics for the two aforementioned concordance indicators are reported in Table 4. With a minimum value of 85.5%, it is clear that the concordance between the two participants is very strong. Consequently, our indicators of real-time traffic density are reliable.

3.3. Bayesian models: Factors associated with exposure

3.3.1. Assessment of the models

The results of the four Bayesian models are reported in Tables 5 and 6. Before entering into a detailed analysis of the four models, it should be noted that the temperature was excluded due to excessive collinearity with humidity ($R^2 = -0.974$). All models' parameters converged (Rhat = 1.0) and all the trace plots display important mixing (four chains) (Figures S1, S2 and S3, supplementary material). The posterior predictive checks demonstrate that the three models are well fitted (Figure S4, supplementary material). Also, the autocorrelation function (ACF) values calculated on the residuals suggest that there is no temporal dependency in the four models (Table S2, supplementary material).

Table 5. Results of the Bayesian models for the noise exposure

	Model A[1]		Model B[1]	
	Est.	95% CI	Est.	95% CI
Fixed effects				
(Intercept)	73.34	[69.24 77.18]	71.62	[67.92 75.45]
Humidity (%)	0.07	[−0.04 0.18]	0.06	[−0.05 0.16]
Speed (km/h)	0.07	[−0.05 0.07]	0.04	[−0.02 0.09]
Slope (%)	0.04	[−0.04 0.12]	0.03	[−0.05 0.11]
Intersections crossed	0.04	[−0.14 0.22]	0.05	[−0.12 0.22]
Trunk road	Ref		Ref	
Primary road	−1.95	[−3.81 0.10]	−2.12	[−3.94 −0.29]
Secondary road	−4.64	[−6.53 −2.71]	−4.33	[−6.24 −2.44]
Tertiary road	−4.34	[−6.39 −2.29]	−4.28	[−6.25 −2.29]
Residential street	−6.29	[−8.23 −4.38]	−5.51	[−7.39 −3.64]
Pedestrian path or Footway	−10.27	[−14.08 −6.40]	−9.40	[−13.22 −5.60]
Cycleway	−4.87	[−6.90 −2.80]	−4.21	[−6.22 −2.22]
Cycle track or bike lane	−1.32	[−3.36 −0.74]	−1.21	[−3.20 −0.79]
Major road within a distance of 25 metres of the cycleway				
Motorway (dummy)	1.49	[−0.11 3.09]	0.96	[−0.57 2.50]
Trunk (dummy)	1.90	[0.38 3.38]	1.80	[0.39 3.22]
Primary road (dummy)	0.72	[−0.38 1.82]	0.34	[−0.70 1.40]
Secondary road (dummy)	0.75	[−0.39 1.88]	0.22	[−0.88 1.34]
Moving cars × 10			0.35	[0.18 0.52]
Moving heavy vehicles × 10			2.67	[1.21 4.14]

Table 5 – (continued)

	Model A[1]		Model B[1]	
	Est.	95% CI	Est.	95% CI
Random effects (intercept)				
Monday	0.15	[−0.73 1.47]	0.17	[−0.70 1.48]
Tuesday	0.03	[−1.00 1.19]	−0.02	[−1.06 1.07]
Thursday	0.02	[−0.94 1.07]	−0.09	[−1.14 0.86]
Friday	−0.01	[−1.09 1.13]	0.07	[−0.91 1.27]
Moving average				
MA[1]	0.42	[0.33 0.50]	0.40	[0.31 0.48]
MA[2]	0.04	[−0.05 0.13]	0.05	[−0.05 0.14]
MA[3]	0.02	[−0.08 0.12]	0.03	[−0.07 0.12]
Bayes marginal R-squared	0.352	[0.306 0.396]	0.398	[0.356 0.437]
Bayes conditional R-squared	0.351	[0.305 0.394]	0.397	[0.356 0.335]
Waic	3453.3		3396.0	
looic	3453.5		3396.3	

Estimate and 95% CI adjusted for the time of day (spline on the number of minutes passed since 08:00) and location (bivariate spline on the geographic coordinates).

The values of Bayes marginal and conditional R-squared are very similar for the noise exposure models (Table 5), but very different for the NO_2 exposure models (Table 6). This implies that the day of the week introduced as a random effect only plays an important role in the NO_2 exposure models. As a result, the intercepts of the random effects vary significantly according to the day of the week for the NO_2 exposure models, but they are not significant for the noise exposure models. This means that the noise levels measured are broadly similar for the four days of collection. Of course, this observation only applies to our data collection week and it cannot be generalized to the whole year. However, these results demonstrate the relevance of introducing the day of the week as a random effect in order to obtain unbiased coefficients for the fixed effects predictors.

Table 6. Results of the Bayesian models for the NO$_2$ exposure

	Model A[1]		Model B[1]	
	Est.	95% CI	Est.	95% CI
Fixed effects				
(Intercept)	240.41	[180.00 300.14]	241.57	[179.35 300.96]
Humidity (%)	−0.66	[−2.38 1.05]	−0.64	[−2.34 1.11]
Speed (km/h)	0.19	[−0.10 0.47]	0.16	[−0.13 0.45]
Slope (%)	0.23	[−0.14 0.60]	0.23	[−0.14 0.60]
Intersections crossed	−0.10	[−0.95 0.75]	−0.13	[−1.00 0.74]
Trunk road	Ref		Ref	
Primary road	−12.17	[−1.77 −0.46]	−11.41	[−20.92 −1.75]
Secondary road	−13.64	[−3.64 −2.32]	−13.40	[−23.04 −3.74]
Tertiary road	−11.45	[−5.67 −2.88]	−11.39	[−21.52 −0.98]
Residential street	−10.97	[−5.35 −4.02]	−11.35	[−21.16 −1.68]
Pedestrian path or Footway	−26.90	[−4.84 −2.76]	−27.18	[−44.34 −9.68]
Cycleway	−11.26	[−4.84 −3.19]	−11.42	[−21.48 −1.40]
Cycle track or bike lane	−3.81	[−1.74 −0.03]	−4.22	[−15.98 7.31]
Major road within a distance of 25 metres of the cycleway				
Motorway (dummy)	6.78	[−0.30 13.74]	6.93	[0.07 13.88]
Trunk (dummy)	9.38	[2.15 16.48]	9.59	[2.45 16.78]
Primary road (dummy)	2.89	[−2.43 8.33]	3.14	[−2.18 8.51]
Secondary road (dummy)	−0.55	[−5.98 4.84]	−0.38	[−5.69 4.94]
Total cars × 10			−0.47	[−1.24 0.31]
Total heavy vehicles × 10			0.31	[−4.68 5.33]

Table 6 – (continued)

	Model A[1]		Model B[1]	
	Est.	95% CI	Est.	95% CI
Random effects (intercept)				
Monday	31.91	[6.27 61.65]	31.68	[6.06 61.44]
Tuesday	33.30	[9.40 61.23]	33.02	[9.42 60.74]
Thursday	−9.57	[−30.66 14.31]	−9.55	[−30.47 13.72]
Friday	−17.28	[−40.81 6.71]	−17.57	[−41.34 5.93]
Moving average				
MA[1]	0.82	[0.73 0.91]	0.82	[0.73 0.91]
MA[2]	0.40	[0.30 0.50]	0.40	[0.30 0.50]
MA[3]	0.11	[0.03 0.20]	0.12	[0.04 0.20]
Bayes marginal R-squared	0.841	[0.809 0.865]	0.842	[0.809 0.866]
Bayes conditional R-squared	0.888	[0.880 0.895]	0.888	[0.879 0.895]
Waic	5659.0		5662.0	
looic	5659.7		5662.9	

Estimate and 95% CI adjusted for the time of day (spline on the number of minutes passed since 08:00) and location (bivariate spline on the geographic coordinates).

As mentioned before, to meet the third objective – to evaluate the influence of real-time traffic density on cyclists' exposure –, two different models were estimated: a first model with predictors related to the type of road and bicycle path taken by the cyclist (Models A, Tables 5 and 6), and a second model in which were added the predictors related to real-time traffic density (Models B, Tables 5 and 6). For the noise exposure prediction, the goodness of fit (Bayes conditional R-squared, Waic, looic) between model A and model B indicates that the introduction of the real-time traffic density predictors significantly improves the model. However, this finding does not apply to the NO_2 exposure prediction since the differences between the fit statistics are very weak.

3.3.2. Analysis of the fixed linear terms

At the outset, it is worth noting the coefficients obtained for both models (A and B) are very similar (Tables 5 and 6). For reasons of parsimony, we will then present only those of the final models (B). With respect to the control variables, humidity, speed, slope and number of intersections crossed have a not significant effect on noise and NO_2 exposure in any model (Tables 5 and 6).

Unsurprisingly, exposure to road traffic noise and nitrogen dioxide are strongly associated with the type of road or bicycle infrastructure taken by the cyclist. Compared with the time spent travelling on a trunk road (reference category), taking other types of roads significantly reduces the cyclist's exposure to noise and air pollution. For noise, the levels of exposure are especially lower on pedestrian paths or footways, residential streets and cycleways (-9.4, -5.5, -4.2 dB(A) for noise and -27.2, -11.4, -11.4 $\mu g/m^3$ for NO_2 respectively). In contrast, taking a cycle track or a shared lane has a low impact on reducing the exposure to road traffic noise (-1.2 dB(A)) and NO_2 (-4.2 $\mu g/m^3$).

The type of road nearby the cycleway (*i.e.*, off-street or on-street bicycle path) within a 25-metre radius also had significant impacts on the exposure. For example, the presence of a section of motorway or trunk road near the bicycle path significantly increased exposure to noise (0.96 and 1.8 dB(A)) and NO_2 (6.93 and 9.59 $\mu g/m^3$). On the other hand, presences within 25 metres of a primary or secondary road were not significantly associated with higher levels of exposure.

Finally, the real-time traffic density coefficients are significant for the noise exposure (Model B, Table 5), but not for the NO_2 exposure. Indeed, per 10 heavy vehicles encountered each minute by the cyclist, we found an increase of 2.67 dB(A) in road traffic noise exposure *versus* 0.35 dB(A) increase for 10 moving cars.

4. Discussion

4.1. Limitations of the study

Although the size of the data set was large enough to enable us to perform rigorous statistical analyses (n = 630), it is important to remember that it only included 137 kilometres and 11 hours of data collection. Some recent studies with similar approaches have used fairly sizeable data sets: for example, 422 km and 22 hours of collection in Montreal (Apparicio *et al*., 2016), 964 and 64 hours in Paris (Gelb and Apparicio, 2020) and, 27 hours in eleven Dutch cities (Boogaard *et al*., 2009). In our case, because it was quite a long and onerous task for the two participants to count the vehicles on the videos, we chose to conduct a study on a rather limited sample. Since the contribution of the traffic indicators has proven to be conclusive, it would therefore be appropriate to apply this to larger samples and for other cities as well. To estimate the traffic encountered along the route, we only used one camera attached to the bicycle's handlebars. In future works, it could be relevant to use a second camera to count vehicles behind the cyclist.

4.2. The effects of real-time traffic measures

We found that variables introduced to control for the traffic encountered by cyclists had a significant positive effect on noise exposure, and a positive but not significant effect on NO_2 exposure. This can be explained in particular by the fact that noise is an immediate pollutant, which is dispersed in the air directly after being generated. Conversely, air pollution can accumulate over time, so that the importance of real-time traffic variables is more relative. In other words, what is important from the point of view of NO_2 exposure on a road is not the number of vehicles encountered within one minute, but rather the number of vehicles that have already travelled on that road since the beginning of the day. That explains the road type has clearly a significant important on exposure to NO_2. It would be very interesting to complement these results by including annual average daily traffic flows, as that variable could more effectively capture this notion of pollution accumulation.

5. Conclusion

The analysis of the collected data has revealed that the levels of exposure to road traffic noise and NO_2 are especially high for cyclists in Mexico City. The type of road or bicycle infrastructure taken by the cyclist has both significant impacts on exposure to noise and air pollution. Taking residential streets and cycle paths away from major rather than major roads significantly reduces the cyclist's exposure to noise and air pollution. This is good news for two reasons. First, when possible, the cyclists could significantly reduce their noise exposure by modifying their routes. Second, the bicycle infrastructure planners could have a significant impact on cyclists' exposure by implementing new cycling routes in a less noisy or air-polluted urban environment. The inclusion of real-time traffic indicators constructed by using videos taken by an action camera fixed onto the cyclist's handlebars has thus proven to be a good way of modelling levels of exposure. So it would be worth repeating this exercise in other urban contexts and for other air pollutants (*e.g.* particulate matters – $PM_{2.5}$). This would lead a better understand the complex relationships between traffic, noise exposure, and exposure and inhalation of air pollutants.

References

Apparicio P., Carrier M., Gelb J., Séguin A.-M., Kingham S. (2016). Cyclists' exposure to air pollution and road traffic noise in central city neighbourhoods of Montreal. *Journal of Transport Geography*, vol. 57, p. 63-69.

Apparicio P., Gelb J. (2020). Cyclistsʹ exposure to road traffic noise: A comparison of three North American and European cities. *Acoustics*, vol. 2, p. 73-86.

Apparicio P., Gelb J., Carrier M., Mathieu M.-È., Kingham S. (2018). Exposure to noise and air pollution by mode of transportation during rush hours in Montreal. *Journal of Transport Geography*, vol. 70, p. 182-192.

Apparicio P., Maignan D., Gelb J. (2021). VIFECO: An Open-Source Software for counting features on a video. *Journal of Open Research Software*, vol. 9, p. 1-9.

Apparicio P., Gelb J., Mathieu M.-E. (2019). Un atlas-web pour comparer l'exposition individuelle aux pollutions atmosphérique et sonore selon le mode de transport. *Cybergeo: European Journal of Geography*, 309.

Bassett D. R., Pucher Jr J., Buehler R., Thompson D.L., Crouter S.E. (2008). Walking, cycling, and obesity rates in Europe, North America, and Australia. *Journal of Physical Activity and Health*, vol. 5, n° 6, p. 795-814.

Bigazzi A.Y., Figliozzi M.A. (2014). Review of Urban Bicyclists' Intake and Uptake of Traffic-Related Air Pollution. *Transport Reviews*, vol. 34, n° 2, p. 221-245.

Boogaard H., Borgman F., Kamminga J., Hoek G. (2009). Exposure to ultrafine and fine particles and noise during cycling and driving in 11 Dutch cities. *Atmospheric Environment*, vol. 43, n° 27, p. 4234-4242.

Buehler R., Pucher J. (2012). International Overview: Cycling Trends in Western Europe, North America, and Australia.*City cycling*, Cambridge, Masschusetts, The MIT Press, p. 9-29.

Bürkner P.-C. (2017). brms: An R package for Bayesian multilevel models using Stan. *Journal of Statistical Software*, vol. 80, n° 1, p. 1-28.

Bürkner P.-C. (2018). Advanced Bayesian multilevel modeling with the R package brms. *The R Journal*, vol. 10, n° 1, p. 395-411.

Cepeda M., Schoufour J., Freak-Poli R., Koolhaas C.M., Dhana K., Bramer W.M., Franco O.H. (2017). Levels of ambient air pollution according to mode of transport: a systematic review. *The Lancet Public Health*, vol. 2, n° 1, p. e23-e34.

Ciudad de México (2017). *CDMX: Hacia una ciudad ciclista*. México City

Contributors OpenStreetMap (2017). Planet dump retrieved from https://planet.osm.org

Costa S., Ferreira J., Silveira C., Costa C., Lopes D., Relvas H., Borrego C., Roebeling P., Miranda A.I., Paulo Teixeira J. (2014). Integrating health on air quality assessment - review report on health risks of two major European outdoor air pollutants: PM and NO2. *Journal of Toxicology and Environmental Health, Part B*, vol. 17, n° 6, p. 307-340.

Crouse D.L., Goldberg M.S., Ross N.A. (2009). A prediction-based approach to modelling temporal and spatial variability of traffic-related air pollution in Montreal, Canada. *Atmospheric Environment*, vol. 43, n° 32, p. 5075-5084.

De Hartog J.J., Boogaard H., Nijland H., Hoek G. (2010). Do the health benefits of cycling outweigh the risks? *Environmental Halth Perspectives*, vol. 118, n° 8, p. 1109-1116.

Delgado-Saborit J.M. (2012). Use of real-time sensors to characterise human exposures to combustion related pollutants. *Journal of Environmental Monitoring*, vol. 14, n° 7, p. 1824-1837.

Deville Cavellin L., Weichenthal S., Tack R., Ragettli M.S., Smargiassi A., Hatzopoulou M. (2016). Investigating the use of portable air pollution sensors to capture the spatial variability of traffic-related air pollution. *Environmental Science & Technology*, vol. 50, n° 1, p. 313-320.

Dill J., Carr T. (2003). Bicycle commuting and facilities in major US cities: if you build them, commuters will use them. *Transportation Research Record: Journal of the Transportation Research Board*, n° 1828, p. 116-123.

Dons E., Panis L.I., Van Poppel M., Theunis J., Wets G. (2012). Personal exposure to black carbon in transport microenvironments. *Atmospheric Environment*, vol. 55, p. 392-398.

Fishman E., Schepers P., Kamphuis C.B.M. (2015). Dutch cycling: quantifying the health and related economic benefits. *American Journal of Public Health*, vol. 105, n° 8, p. e13-e15.

Gelb J., Apparicio P. (2019). Noise exposure of cyclists in Ho Chi Minh City: A spatio-temporal analysis using non-linear models. *Applied Acoustics*, vol. 148, p. 332-343.

Gelb J., Apparicio P. (2020). Modelling Cyclists' Multi-Exposure to Air and Noise Pollution with Low-Cost Sensors - The Case of Paris. *Atmosphere*, vol. 148, p. 332-343.

Gelman A. (2006). Prior distributions for variance parameters in hierarchical models (comment on article by Browne and Draper). *Bayesian Analysis*, vol. 1, n° 3, p. 515-534.

Gobierno del Distrito Federal (2011). *Estrategia de movilidad en bicicleta de la Ciudad de México, Secretaría del medio ambiente*. México, Secretaría del medio ambiente.

Gobierno del Distrito Federal (2017). Agenda ambiental de la Ciudad de México.Programa del Medio ambiente 2007-2012. México, Secretaría del medio ambiente.

Gustafson P., Hossain S., Macnab Y.C. (2006). Conservative prior distributions for variance parameters in hierarchical models. *Canadian Journal of Statistics*, vol. 34, n° 3, p. 377-390.

Hall A., Thebault-Spieker J., Sen S., Hecht B., Terveen L. (2001). Exploring the Relationship Between "Informal Standards" and Contributor Practice in OpenStreetMap.*Actes du colloque OpenSym '18 (14th International Symposium on Open Collaboration)*, Association for Computing Machinery, New York.

Hatzopoulou M., Weichenthal S., Dugum H., Pickett G., Miranda-Moreno L., Kulka R., Andersen R., Goldberg M. (2013). The impact of traffic volume, composition, and road geometry on personal air pollution exposures among cyclists in Montreal, Canada. *Journal of Exposure Science & Environmental Epidemiology*, vol. 23, n° 1, p. 46-51.

Jarvis A., Reuter H.I., Nelson A., Guevara E. (2008). Hole-filled SRTM for the globe Version 4. *International Centre for Tropical Agriculture (CIAT). http://srtm.csi.cgiar.org*

Khan J., Ketzel M., Kakosimos K., Sørensen M., Jensen S.S. (2018). Road traffic air and noise pollution exposure assessment - A review of tools and techniques. *Science of the Total Environment*, vol. 634, p. 661-676.

Khaniabadi Y.O., Goudarzi G., Daryanoosh S.M., Borgini A., Tittarelli A., De Marco A. (2017). Exposure to PM10, NO2, and O3 and impacts on human health. *Environmental Science and Pollution Research*, vol. 24, n° 3, p. 2781-2789.

Leo A., Morillón D., Silva R. (2017). Review and analysis of urban mobility strategies in Mexico. *Case Studies on Transport Policy*, vol. 5, n° 2, p. 299-305.

Lin C., Gillespie J., Schuder M., Duberstein W., Beverland I., Heal M. (2015). Evaluation and calibration of Aeroqual series 500 portable gas sensors for accurate measurement of ambient ozone and nitrogen dioxide. *Atmospheric Environment*, vol. 100, p. 111-116.

Luxen D., Vetter C. (2011). *Real-time routing with OpenStreetMap data*, ACM.

Minet L., Gehr R., Hatzopoulou M. (2017). Capturing the sensitivity of land-use regression models to short-term mobile monitoring campaigns using air pollution micro-sensors. *Environmental Pollution*, vol. 230, p. 280-290.

Mooney P., Corcoran P. (2012). Characteristics of heavily edited objects in OpenStreetMap. *Future Internet*, vol. 4, n° 1, p. 285-305.

Morawska L., Thai P.K., Liu X., Asumadu-Sakyi A., Ayoko G., Bartonova A., Bedini A., Chai F., Christensen B., Dunbabin M., Gao J., Hagler G.S.W., Jayaratne R., Kumar P., Lau A.K.H., Louie P.K.K., Mazaheri M., Ning Z., Motta N., Mullins B., Rahman M.M., Ristovski Z., Shafiei M., Tjondronegoro D., Westerdahl D., Williams R. (2018). Applications of low-cost sensing technologies for air quality monitoring and exposure assessment: How far have they gone? *Environment International*, vol. 116, p. 286-299.

Oja P., Vuori I., Paronen O. (1998). Daily walking and cycling to work: their utility as health-enhancing physical activity. *Patient Education and Counseling*, vol. 33, p. S87-S94

Ouyang W., Guo B., Cai G., Li Q., Han S., Liu B., Liu X. (2015). The washing effect of precipitation on particulate matter and the pollution dynamics of rainwater in downtown Beijing. *Science of the Total Environment*, vol. 505, p. 306-314.

Pucher J., Buehler R., Seinen M. (2011). Bicycling renaissance in North America? An update and re-appraisal of cycling trends and policies. *Transportation Research Part A: Policy and Practice*, vol. 45, n° 6, p. 451-475.

Reuter H.I., Nelson A., Jarvis A. (2007). An evaluation of void-filling interpolation methods for SRTM data. *International Journal of Geographical Information Science*, vol. 21, n° 9, p. 983-1008.

Ríos Flores R.A., Taddia A.P., Pardo C., Lleras N. (2015). *Ciclo-inclusión en América Latina y el Caribe: Guía para impulsar el uso de la bicicleta*. https://publications.iadb.org/handle/11319/6808

Rojas-Rueda D., de Nazelle A., Tainio M., Nieuwenhuijsen M.J. (2011). The health risks and benefits of cycling in urban environments compared with car use: health impact assessment study. *Bmj*, vol. 343, p. 1-8.

Rosas-Satizábal D., Rodriguez-Valencia A. (2019). Factors and policies explaining the emergence of the bicycle commuter in Bogotá. *Case Studies on Transport Policy*, vol. 7, n° 1, p. 138-149.

Secretaría de Medio Ambiente y Recursos Naturales (2013). *Norma Oficial Mexicana NOM-081-SEMARNAT-1994. Que establece los límites máximos permisibles de emisión de ruido de las fuentes fijas y su método de medición*. Diario Oficial de la Federación.

Snyder E.G., Watkins T.H., Solomon P.A., Thoma E.D., Williams R.W., Hagler G.S., Shelow D., Hindin D.A., Kilaru V.J., Preuss P.W. (2013). *The changing paradigm of air pollution monitoring*, ACS Publications.

Sueur J., Aubin T., Simonis C. (2008). Seewave, a free modular tool for sound analysis and synthesis. *Bioacoustics*, vol. 18, n° 2, p. 213-226.

Tainio M., de Nazelle A.J., Götschi T., Kahlmeier S., Rojas-Rueda D., Nieuwenhuijsen M.J., de Sá T.H., Kelly P., Woodcock J. (2016). Can air pollution negate the health benefits of cycling and walking? *Preventive Medicine*, vol. 87, p. 233-236.

Team R Core (2017). *R: A Language and Environment for Statistical Computing*, Vienna, Austria, https://www.R-project.org/

Teschke K., Harris M.A., Reynolds C.C., Winters M., Babul S., Chipman M., Cusimano M.D., Brubacher J.R., Hunte G., Friedman S.M. (2012). Route infrastructure and the risk of injuries to bicyclists: a case-crossover study. *American Journal of Public Health*, vol. 102, n° 12, p. 2336-2343.

Tucker B., Manaugh K. (2018). Bicycle equity in Brazil: Access to safe cycling routes across neighborhoods in Rio de Janeiro and Curitiba. *International Journal of Sustainable Transportation*, vol. 12, n° 1, p. 29-38.

Vallejo M., Lerma C., Infante O., Hermosillo A.G., Riojas-Rodriguez H., Cárdenas M. (2004). Personal exposure to particulate matter less than 2.5 μm in Mexico City: a pilot study. *Journal of Exposure Science and Environmental Epidemiology*, vol. 14, n° 4, p. 323-329.

Wood S.N., Pya N., Säfken B. (2016). Smoothing Parameter and Model Selection for General Smooth Models. *Journal of the American Statistical Association*, vol. 111, n° 516, p. 1548-1563.

Woodcock J., Edwards P., Tonne C., Armstrong B.G., Ashiru O., Banister D., Beevers S., Chalabi Z., Chowdhury Z., Cohen A. (2009). Public health benefits of strategies to reduce greenhouse-gas emissions: urban land transport. *The Lancet*, vol. 374, n° 9705, p. 1930-1943.

World Health Organization (2006). *WHO Air quality guidelines for particulate matter, ozone, nitrogen dioxide and sulfur dioxide: global update 2005: summary of risk assessment*, Geneva, World Health Organization, 2006.

World Health Organization (2018). *Environmental Noise Guidelines for the European Region*, 2018.